Journal of ELECTRONIC MATERIALS, Vol. 36, No. 2, 2007 *Regular Issue Paper*
DOI: 10.1007/s11664-006-0060-x
© 2007 TMS

Three-Dimensional Thermoelectrical Simulation in Flip-Chip Solder Joints with Thick Underbump Metallizations during Accelerated Electromigration Testing

S.W. LIANG,[1] Y.W. CHANG,[1] and CHIH CHEN[1,2]

1.—Department of Material Science and Engineering, National Chiao Tung University, Taiwan, Republic of China. 2.—E-mail: chih@faculty.nctu.edu.tw

In flip-chip solder joints, thick Cu and Ni films have been used as under bump metallization (UBM) for Pb-free solders. In addition, electromigration has become a crucial reliability concern for fine-pitch flip-chip solder joints. In this paper, the three-dimensional (3-D) finite element method was employed to simulate the current-density and temperature distributions for the eutectic SnPb solder joints with 5-μm Cu, 10-μm Cu, 25-μm Cu, and 25-μm Ni UBMs. It was found that the thicker the UBM is the lower the maximum current density inside the solder. The maximum current density is 4.37×10^4 A/cm^2, 1.69×10^4 A/cm^2, 7.54×10^3 A/cm^2, and 1.34×10^4 A/cm^2, respectively, when the solder joints with the above four UBMs are stressed by 0.567 A. The solder joints with thick UBMs can effectively relieve the current crowding effect inside the solder. In addition, the joint with the thicker Cu UBM has a lower Joule heating effect in the solder. The joint with the 25-μm Ni UBM has the highest Joule heating effect among the four models.

Key words: Flip chip solder joint, under bump metallization, electromigration, simulation

INTRODUCTION

The flip-chip solder joint has become the most important technology for high-density packaging in the microelectronic industry.[1] As the required performance in microelectronics devices becomes higher, thousands of solder bumps are fabricated into one chip. Thus, the size of the joints progressively shrinks. Their diameter is about 100 μm or less.[2] The design rule of packaging requires that each bump is going to carry 0.2 to 0.4 A, resulting in a current density of approximately 2×10^3 to 2×10^4 A/cm^2. Therefore, electromigration has become an important reliability issue for flip-chip solder joints.[3–5]

Due to the special line-to-bump geometry of the flip-chip solder joints, serious current crowding occurs in the entrance point of the Al trace into the bump during current stressing.[6,7] In addition, serious Joule heating may occur in the solder joints when stressed at high current.[8] Therefore, solder near the entrance point may be migrated away and voids thus form there.[9] The current crowding effect plays a crucial role in the failure of joints. Previous modeling results and experimental data show that the solder joints with thin-film under-bump metallization (UBM) have shorter failure time due to higher current crowding effect in the solder.[10,11] The maximum current density inside the solder with Al/Ni(V)/Cu thin-film UBM may be 22.2 times larger than the average value, and the average temperature in the solder is 98.8 when the solder joints are applied by 0.567 A at 70°C.[12]

Moreover, thick electroplated Cu and electroless Ni have been adopted for the UBM of Pb-free solders due to metallurgical reliability concerns. However, the current-density and temperature distribution in the flip-chip solder joints with thick-film UBMs during electromigration is not clear. Thick-film UBM may have better ability to relieve the current crowding effect and Joule heating effect. In this paper, we employed a three-dimensional (3-D) finite element method to model the current-density and temperature distributions in the solder joints with 5-μm Cu, 10-μm Cu, 25-μm Cu, and 25-μm Ni UBMs. The mechanism of how the thick UBM could relieve the current crowding and Joule heating

(Received June 20, 2006; accepted October 24, 2006)

effect was proposed. The effect of current crowding and Joule heating on mean-time-to-failure is discussed. This research provides a deeper understanding on the current density and temperature distribution in the solder joints with thick-film UBM.

SIMULATION

The cross-sectional schematic model is shown in Fig. 1a. A simplified UBM structure with an opening of 120 μm in diameter was used. The contact opening on the substrate side is 144 μm in diameter. The dimensions of the Al trace are 34-μm wide and 1.5-μm thick, whereas the Cu line on the substrate side is 80-μm wide and 25-μm thick. The intermetallic compound (IMC) formed between the UBM and the solder was also considered in the simulation models. The electroplated Cu layer was assumed to consume 0.5 μm and to form 1.4 μm of Cu_6Sn_5 IMC. The electroless Ni layer was assumed to consume 0.5 μm and to form 1.0 μm of Ni_3Sn_4 IMC. On the substrate side, a Ni_3Sn_4 IMC of 1 μm was adopted for the Ni metallization. Layered IMCs were used in this simulation for both the Cu_6Sn_5 and Ni_3Sn_4 to avoid difficulty in meshization. In addition, eutectic solder was used in this model. The resistivity and thermal conductivity values of the materials used in the simulation are listed in Table I. The effect of the temperature coefficient of resistivity (TCR) was considered, and the TCR values for the metals are also listed in Table I. However, the thermal conductivity of the electroless Ni could not be found in the literature. The following equation was used to estimated the thermal conductivity.[13]

$$\frac{\kappa}{\sigma}\frac{1}{T} = 3\left(\frac{k}{e}\right)^2$$

where κ is the thermal conductivity; σ is the conductivity; T means the temperature; and k and e are the Boltzmann constant and electron charge, respectively. When the resistivity of electroless Ni with 10% P is 70 $\mu\Omega$-cm, the thermal conductivity is estimated to be 9.3 W/m-°C by this equation.

The model used in this study was a SOLID69 8-node hexahedral coupled field element using ANSYS simulation software. For thermal simulation, we used an infrared microscope to measure the temperature in the solder bumps during current stressing,[8] and then adjusted the simulation parameters so that the simulated temperature in the solder matched the one measured by the infrared microscope under the same applied current.

A 3-D finite element model was constructed to simulate the current density distribution in the flip-chip solder joints, as illustrated in Fig. 1b. A current of 0.567 A was applied. The corresponding current density in the Al trace was 1.11×10^6 A/cm^2, and the calculated average current densities were 5.01×10^3 and 3.48×10^3 A/cm^2 for the contact opening of the chip side and of the substrate side, respectively.

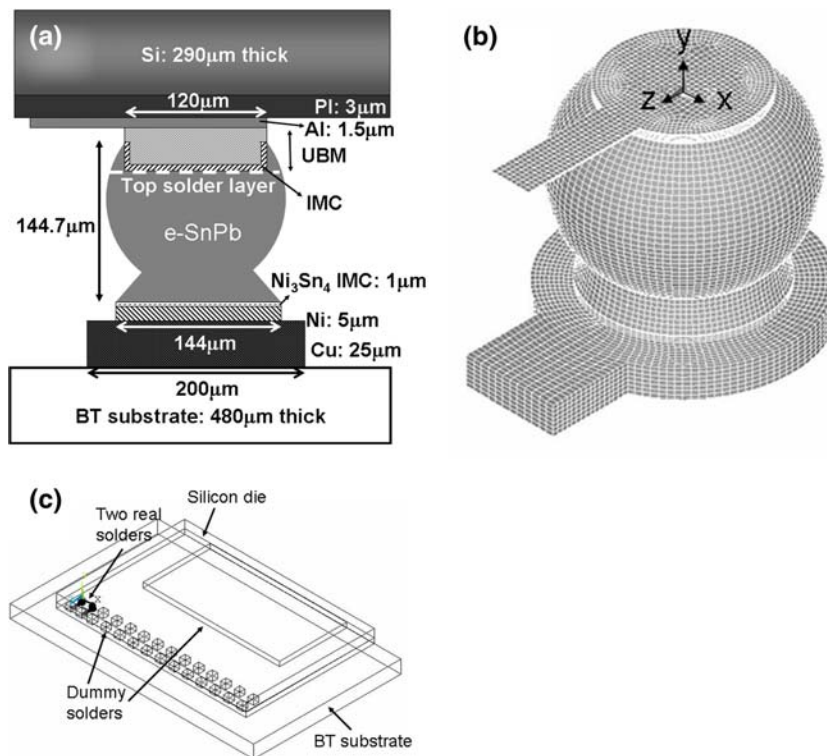

Fig. 1. (a) Schematic drawing of the solder joint with thick-film UBM used in this study. (b) Three-dimensional view of the constructed model with meshization. (c) Constructed flip-chip package for thermal simulation, in which two of the solder joints were subjected to current stressing.

Table I. Properties of Materials Used in the Simulation Models

Materials	Thermal Conductivity (W/m °C)	Resistivity at 20°C (μΩ cm)	TCR (×10^{-3}/K)
Silicon	147.00	—	—
Al trace	238.00	2.7	4.2
Electroless Ni	9.32	70.0	6.8
Cu	403.00	1.7	4.3
Ni	76.00	6.8	6.8
e-SnPb	50.00	14.6	4.4
BT (substrate)	0.70	—	—
Underfill	0.55	—	—
Passivation	0.34	—	—

Figure 1c shows the constructed model for thermal simulation, in which only two solder joints were stressed by current, as indicated by one of the arrows in the figure. The dimension of the Si chip was 7.0 mm × 4.8 mm and the thickness was 290 μm, whereas the dimension of the bismaleimide triazine (BT) substrate was 5.4-mm wide, 9.0-mm long, and 480-μm thick. The bottom of the BT substrate was maintained at 70°C and the convention coefficient was set to 10 W/m^2-°C around the 25°C environment temperature. The current applied on the two solder joints ranged from 0.1 A to 0.567 A.

RESULTS

The current-density distribution in the four solder joints under 0.567 A will be illustrated by two figures, including a 3-D tilt view, a cross-sectional view along the *Z*-axis, and a cross-sectional view on the top solder layer, as depicted by the white dotted line in Fig. 1a. Because voids form and propagate in this layer, the current-density distribution in this layer is very important. The crowding ratio in the paper is denoted as the maximum current density in the solder divided by the average value in the UBM opening, which is 5.01×10^3 A/cm^2. In this paper, we will focus on the current density in the top layer of solder adjacent to the IMC layer, because electromigration failure occurs mainly in solder. The temperature distributions in the solder joints with 25-μm Cu and 25-μm Ni under 0.567 A will be illustrated by two figures, including a 3-D tilt view and a cross-sectional view along the *Z*-axis. In addition, the hot-spot temperature in the solder bump near the entrance point of the Al trace was also extracted. The vertical and horizontal temperature gradients will be presented in this paper.

Current Density Distribution

For the joint with the 5-μm Cu UBM, the maximum current density inside the solder occurs in the entrance point of Al trace into the solder joint, while there is no obvious current crowding effect in the substrate side of the joint, as seen in Fig. 2a. Figure 2a displays the current density distribution at the cross section along the *Z*-axis in Fig. 1b. Once the current enters the solder joint, it drifts down vertically toward the substrate (*Y*-axis direction) and also spreads out laterally at the same time (*X*-axis and *Z*-axis directions). The maximum current density is as high as 4.37×10^4 A/cm^2 at the solder near the entrance of the Al trace. On the substrate side, the current crowding phenomenon is much less due to a larger contact opening and a thicker Cu line. The average current density in the

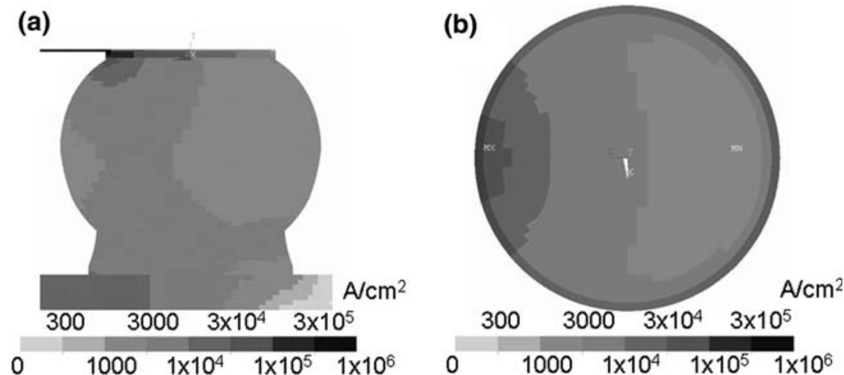

Fig. 2. Current density distribution in the solder joint with the 5-μm Cu UBM: (a) cross-sectional view along the *z*-axis and (b) in the top solder layer.

Cu line is 2.84×10^4 A/cm^2, which is 34 times less than that in the Al trace.

In addition, the current density distribution in the top solder layer connecting to the IMC layer is illustrated in Fig. 2b. It was found that the maximum current density for the cross section is 4.37×10^4 A/cm^2. The current spreads out in the Cu layer, and the current density decreased down to 4.37×10^4 A/cm^2 in the solder layer connecting to the Cu_6Sn_5 IMC. However, the crowding ratio is still 8.7, which means 8.7 times larger than the average value in the UBM opening.

The thickness of the Cu UBM increased to 10 μm, as shown in Fig. 3a. However, the current crowding still occurred near the entrance point of the Al trace in the solder joint. The current density in the solder was relieved to some extent, as shown in Fig. 3b. The maximum current density in the top solder layer decreased to 1.69×10^4 A/cm^2. Compared with the value in the solder bump with 5-μm Cu, which had a maximum current density of 4.37×10^4 A/cm^2 in the top solder layer, it was reduced by a factor of 3.4. This indicates that thicker Cu UBM may render a lower current crowding effect.

The current crowding effect inside the solder was further relieved when the thickness of the Cu UBM increased to 25 μm. The current-density distribution in the solder joint is shown in Fig. 4a. Although the current crowding effect still occurred in the vicinity of the entrance point of the Al trace, the maximum current density in the top layer of the solder was further reduced down 7.54×10^3 A/cm^2, and the corresponding crowding ratio was only 1.5. As shown in Fig. 4a and b, the current distributes almost uniformly inside the solder.

When the 25-μm electroless Ni was adopted, the current-density distribution in the solder joint was as shown in Fig. 5a and b. The maximum current density for the top layer of the solder was 1.34×10^4 A/cm^2, and the corresponding crowding ratio was 2.7. Compared to the solder joints with 25-μm Cu UBM in Fig. 4a, the current crowding effect in the entrance of the Al trace was less serious, but the maximum current density in the top solder layer of the solder was 1.8 times larger than that in the joint with 25-μm Cu UBM. The current-density distribution in the lower part of the bump did not change much as the thickness of the UBM changed.

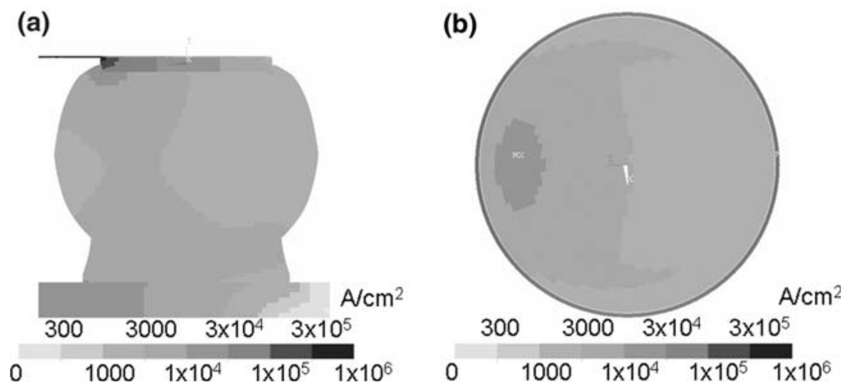

Fig. 3. Current density distribution in the solder joint with the 10-μm Cu UBM: (a) cross-sectional view along the z-axis and (b) in the top solder layer.

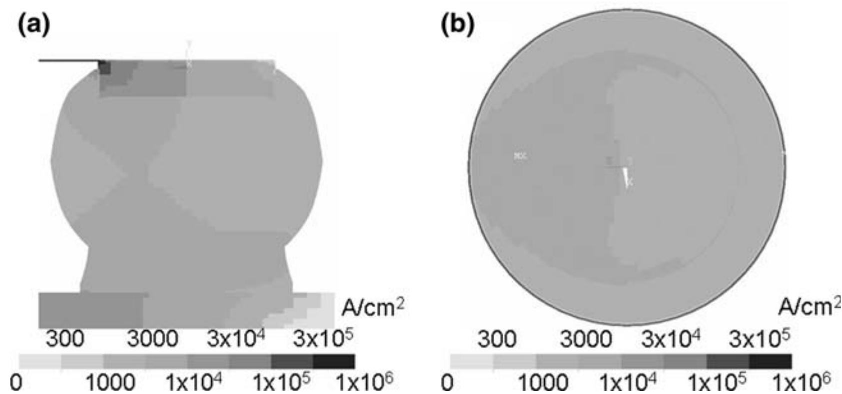

Fig. 4. Current density distribution in the solder joint with the 25-μm Cu UBM: (a) cross-sectional view along the z-axis and (b) in the top solder layer.

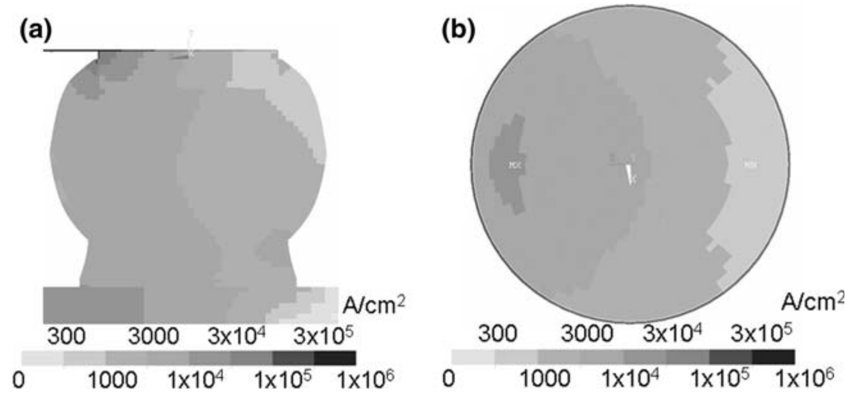

Fig. 5. Current density distribution in the solder joint with 25-μm electroless Ni UBM: (a) cross-sectional view along the z-axis and (b) in the top solder layer.

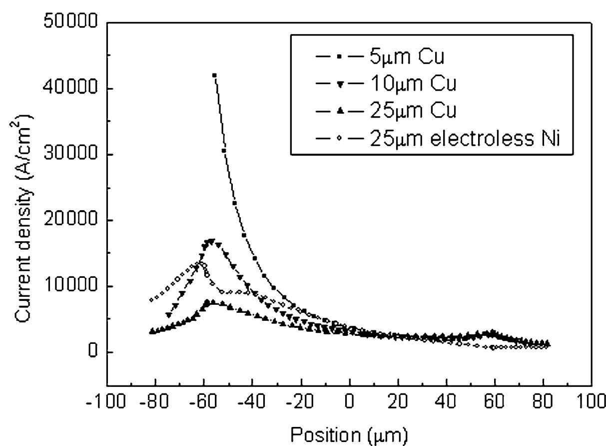

Fig. 6. Current density distribution along the Z-axis on the top solder layer for the four models.

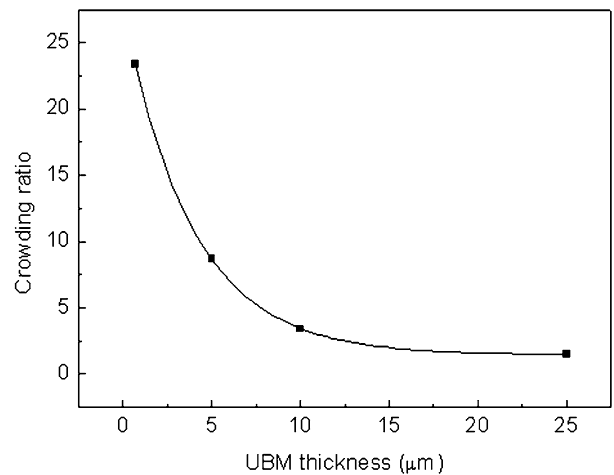

Fig. 7. Plot of crowding ratio against the thickness of the Cu UBM.

Figure 6 summarizes the current-density distribution as a function of applied current in the Z-axis in the top solder layer with the four thick-film UBMs in this study. The maximum current densities occurred directly below the entrance of the Al trace, which was located approximately at the position of –60 μm. The current density decreased rapidly away from this location. The maximum current density is 4.37×10^4, 1.69×10^4, 7.54×10^3, and 1.34×10^4 A/cm^2 for the solder joint with 5-μm Cu, 10-μm Cu, 25-μm Cu, and 25-μm Ni UBM, which corresponded to the crowding ratio of 8.7, 3.4, 1.5, and 2.7. Therefore, as the thickness of the Cu UBM increased, the maximum current density in the top layer decreased. Figure 7 plots the crowding ratio against the thickness of the Cu UBM, in which the first point was from our previous publication.[14] It found that the maximum current density in the solder decreased almost exponentially with the increase of the thickness of the Cu UBM. As described above, current crowding occurred in the vicinity of the entrance of the Al trace for the three joints with Cu UBM. The reason thicker Cu UBM could have a lower crowding ratio is that thick Cu UBM kept the solder bump away from the crowding region.

Temperature Distribution

The temperature distributions of the solder joint with the 5-μm Cu UBM under 0.567 amp at 70°C are shown in Fig. 8a. The figure shows the temperature distribution in the solder only. Although the bottom of the BT substrate was maintained at 70°C, the temperature in solder bump was much higher than that due to serious Joule heating in the solder joints. It can be observed that a hot spot exits in the solder near the entrance point of the Al trace. The temperature in the hot spot is 89.5°C. In this paper, the average temperature in the solder was obtained by averaging the values in a 70 μm $\times$ 70 μm area close to the top solder layer, as indicated by the black dotted line in Fig. 8b, which is 87.2°C for this stressing condition. This area covers the central region of the solder bump. In addition, when the area was expanded or shrank slightly, the average temperature did not change much. Thus, it

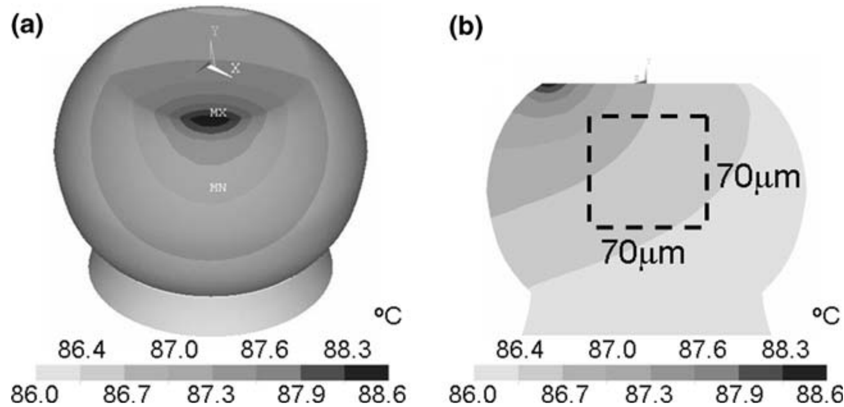

Fig. 8. Temperature distribution in the solder bump with the 5-μm Cu UBM. (a) Three-dimensional tilt view and (b) cross-sectional view along the z-axis. Both figures show the solder only.

is quite representative of its average temperature. The temperature in the hot spot is 2.3°C higher than the average value. The temperature gradient can also be calculated from the temperature distribution. The thermal gradient is denoted to be the temperature difference between the hot spot and the temperature in the bottom solder divided by the bump height. The calculated gradient is 157.4°C/cm for the solder joint with 5-μm Cu UBM under 0.567 A at 70°C. As the thickness of the Cu UBM increased to 25 μm, the average and the hot spot temperatures dropped to 87.0°C and 88.2°C, respectively, as shown in Fig. 9a. Figure 9b illustrates the temperature distribution in the solder bump with the 25-μm Ni UBM. The temperature for the hot spot is 3.3°C higher than that of the joint with the 25-μm Cu UBM. The average temperature is 87.6°C, which is 0.6°C higher than the value in the joint with the 25-μm Cu. To investigate the effect of UBM on the Joule heating effect more thoroughly, various applied currents were simulated. Figure 10a shows the average temperature as a function of applied current to 0.567A for the three models: the joint with 5-μm Cu, 25-μm Cu, and 25-μm Ni UBMs. At applied currents lower than 0.2 A, there was no obvious difference in the temperature in the solder bump. However, as the stressing current increases, the difference becomes more significant. The solder joint with the 25-μm Cu UBM has the lowest Joule heating effect, whereas the one with the 25-μm Ni UBM has the highest Joule heating effect among the three models. In addition, the hot-spot temperature was also examined at various applied currents. Figure 10b shows the hot-spot temperature as a function of applied current. The trend is similar to that of the average temperature, but the temperature difference becomes slightly larger.

The thermal gradient was also investigated at various applied currents, and the results are illustrated in Figure 11. The joint with the 25-μm Cu UBM has the lowest thermal gradient, whereas the solder joint with the 25-μm electroless Ni UBM has the largest thermal gradient. The value is about 290.0°C/cm at 0.567 A. The thermal gradient might be important in terms of thermalmigration.[15] The temperatures and gradients at different applied currents are listed in Tables II and III.

DISCUSSION

As described above, the 25-μm Cu UBM has better ability to reduce the maximum current density in the solder than that in the 25-μm Ni UBM, although the joint with the 25-μm UBM has a more serious current crowding effect in the entrance point of the Al trace. The reason could be the following. As the current reaches the UBM opening, it may keep

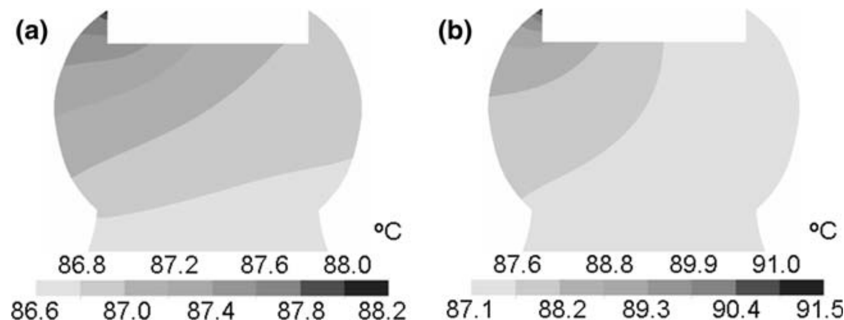

Fig. 9. Cross-sectional view of the temperature distribution for the solder joint with (a) 25-μm Cu and (b) 25-μm Ni.

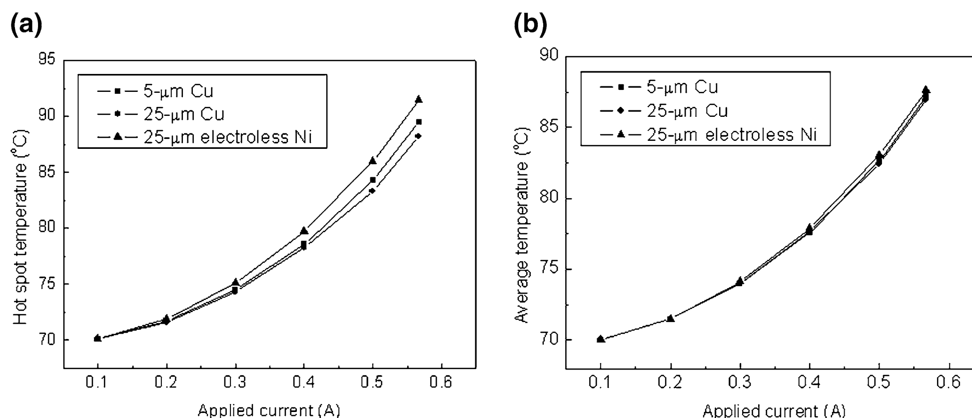

Fig. 10. (a) Average temperature. (b) The hot-spot temperature in the solder bump as a function of applied current up to 0.567 A.

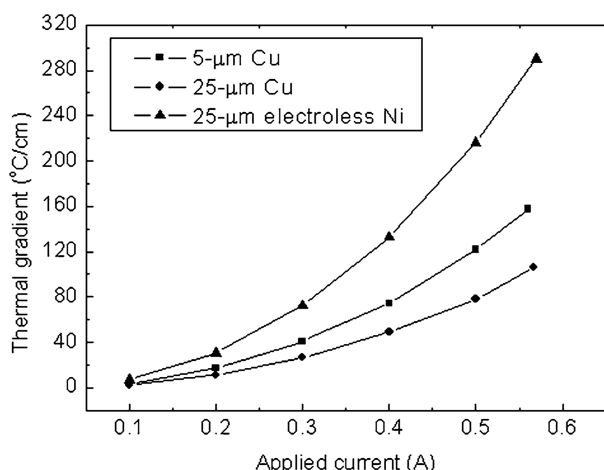

Fig. 11. Thermal gradient in the solder as a function of applied current for 5-μm Cu, 25-μm Cu, and 25-μm electroless Ni UBMs.

drifting straight in the Al pad directly above the UBM or it may drift down toward the substrate side. The ratio depends on the ratio of the resistance of the Al pad to the bump resistance. When the bump resistance is lower than that of the Al trace, more current drifts down in the entrance point rather than continuing to drift straight in the Al pad. For the solder joint with the 25-μm Cu, the bump resistance (3.45 mΩ) is much lower compared with that (11.29 mΩ) with the 25-μm Ni. Thus, the joint with the 25-μm Cu has a more serious current crowding effect in the entrance point, as shown in Figs. 4a and 5a. However, once the current enters the Cu UBM, it spreads out laterally very quickly in the 25-μm Cu due to the lower electrical resistance in the lateral direction, because the Cu has much lower resistivity than that the eutectic solder. Thus, the 25-μm Cu is the best UBM structure to relieve the current crowding effect in this paper.

The reasons that the solder joint with the thick Cu UBM has a lower Joule heating effect may be attributed to the excellent thermal conductivity of Cu and lower local Joule heating in the solder. The major heat source in the joints was the Al trace. Therefore, the thick Cu keeps the solder away from the heat source, and it also helps to dissipate the heat away. In addition, the current density in the solder was much lower than that with thin-film UBM; thus, the local Joule heating is much lower, because the local Joule heating is proportional to the square of local current density. The bump resistance is 4.38 mΩ, 3.84 mΩ, and 3.45 mΩ for the solder joint with 5-μm Cu, 10-μm Cu, and 25-μm Cu, respectively. Thus, the joint with the 25-μm Cu UBM has the lowest average temperature, hot-spot temperature, and thermal gradient. In contrast, the

Table II. Hot-Spot and Average Temperatures in the Solder with the 5-μm Cu, 25-μm Cu, and 25-μm Electroless Ni UBMs

	5-μm Cu UBM		25-μm Cu UBM		25-μm Electroless Ni UBM	
Applied Current (A)	Hot Spot (°C)	Average Temp. (°C)	Hot Spot (°C)	Average Temp. (°C)	Hot Spot (°C)	Average Temp. (°C)
0.1	70.1	70.0	70.1	70.0	70.1	70.0
0.2	71.7	71.5	71.6	71.5	71.9	71.5
0.3	74.5	74.0	74.3	74.0	75.1	74.1
0.4	78.6	77.6	78.3	77.7	79.7	77.9
0.5	84.3	82.6	83.3	82.4	86.0	83.1
0.567	89.5	87.2	88.2	87.0	91.5	87.6

Table III. Thermal Gradients in the Solder Bump with the 5-μm Cu, 25-μm Cu, and 25-μm Electroless Ni UBMs

Applied Current (A)	5-μm Cu UBM Thermal Gradient (°C/cm)	25-μm Cu UBM Thermal Gradient (°C/cm)	25-μm Electroless Ni UBM Thermal Gradient (°C/cm)
0.1	3.7	2.1	7.0
0.2	17.2	11.0	30.3
0.3	40.6	26.4	72.4
0.4	74.2	48.9	133.0
0.5	121.8	77.8	216.2
0.567	157.4	105.8	290.0

joint with the 25-μm Ni UBM has the highest Joule heating effect. The high electrical resistivity of 70 $\mu\Omega$-cm and the low thermal conductivity of 9.3 W/m-°C may be responsible for the poor thermal characteristics of the joint.

Furthermore, the effect of different UBMs on the failure time could be estimated using the equation of mean-time-to-failure (MTTF) for solder joints, which is typically expressed as[16]

$$\mathrm{MTTF} = A\frac{1}{j^n}\exp\left(\frac{Q}{\mathrm{k}T}\right)$$

where A is a constant that contains a factor involving the cross-sectional area of the joint, j is the current density in amperes per square centimeter, n is a model parameter for current density, Q is the activation energy, k is the Boltzmann's constant, and T is the average bump temperature in degrees Kelvin. It is noteworthy that this equation is valid for Al and Cu interconnects, but is questionable if it is applicable in solder joints.[7] Nevertheless, it is still the best equation available to predict the MTTF of the solder joints.[4,17,18]

For the same solder joined to different thicknesses of Cu UBM under the same stressing condition, the values of Q and A are the same. Typically, j represents the average current density calculated on the basis of UBM opening and the applied current. The average current densities are the same for the bumps because they were stressed by the same magnitude of current and the diameters of the UBM opening are identical. The term j^{-n} in the equation needs to be revised to account for the serious current crowding effect in the solder joints. The value of n is equal to 2 for Al lines, and Brandenburg et al. found that n is equal to 1.8 for the eutectic solder joints when the average current density is adopted;[4] the activation energy they measured was 0.8 eV for the SnPb solder with Al/Ni(V)/Cu UBM structure.[7] However, Tu et al. found that it did not fit very well for other bumps.[7] Thus, they proposed that j^{-n} needs to be corrected as $(cj)^{-n}$, in which c is a constant to correct serious current crowding in the solder joints. Further, the T was also modified into $(T + \Delta T)$ to consider the serious Joule heating effect during the accelerated electromigration test. The solder near the entrance of electrons experiences high current density, and thus, higher wind force occurs there. In addition, that solder region also experiences a higher temperature, causing a higher diffusion rate there. Therefore, voids form near the entrance point of the Al trace. Because voids form there, where the solder experiences the maximum current density and the hot-spot temperature, we propose that the (cj) term should be equal to the maximum current density and the hot-spot temperature should be adopted in the $(T + \Delta T)$ term.

The effect of the thick UBM on the MTTF was estimated as follows. Lai et al. reported that the value of n is 0.678, and the activation energy is 0.691 eV for the SnPb solder with Ti/Ni(V)/Cu UBM structure.[19] These values were adopted in the estimation of the MTTF. For the solder joint with Al/Ni(V)/Cu thin-film UBM, the maximum current density is 1.11×10^5 A/cm^2 and the maximum temperature is 98.8°C in the solder, as reported in our previous publications.[14,20] For the solder joint with the 5-μm Cu UBM, the maximum current density was 4.37×10^4 A/cm^2 and the hot-spot temperature was 89.5°C in the solder. The MTTF would be 3.3 times longer than that with the Al/Ni(V)/Cu UBM under 0.567 A at 70°C. For the joint with the 25-μm Cu UBM, the maximum current density decreased to 7.54×10^3 A/cm^2 and the hot-spot temperature was reduced to 88.2°C in the solder. The estimated MTTF would be 11.7 times longer than that of the joint with the Al/Ni(V)/Cu UBM. For the joint with the 25-μm Ni UBM, the MTTF is about 6.5 times longer than the that of the joint with the Al/Ni(V)/Cu UBM if the same activation energy is adopted. The above estimation demonstrates that the solder joints with thicker Cu UBM could significantly increase the electromigration resistance.

CONCLUSIONS

The current density and temperature distributions in the flip-chip solder joints have been carried out by the finite element method. The joint with thick-film Cu UBM has lower maximum current density inside the solder. The crowding ratio in the solder can be reduced down to 1.5 when using a 25-μm Cu UBM. The average and the hot-spot temperatures decreased with the increase of the Cu thickness. The current and temperature spread out more uniformly in the solder joints with the thick-

film Cu UBM. Therefore, the solder joints with the thick Cu UBM were expected to have longer electromigration lifetime.

ACKNOWLEDGEMENTS

The authors thank the National Science Council of the Republic of China for financial support through Grant No. 94-2216-E-009-021. In addition, the assistance of the simulation facility from the National Center for High-Performance Computing (NCHC) in Taiwan is highly appreciated.

REFERENCES

1. Glenn R. Blackwell *The Electronic Packaging Handbook* CRC Press in cooperation with IEEE Press, (Piscataway, NJ, 2000).
2. International Technology Roadmap for Semiconductors Assembly and Packaging Section Semiconductor Industry Association, (San Jose, CA, 2003), pp. 4–9.
3. K.N. Tu, *J. Appl. Phys.* 94, 5451 (2003).
4. S. Brandenburg and S. Yeh *Proc. Surface Mount Int. Conf. Exhib* SMTA, (Edina, MN, 1998), p. 337.
5. C.Y. Liu, Chih Chen, C.N. Liao, and K.N. Tu, *Appl. Phys. Lett.* 75, 58 (1999).
6. C.C. Everett Yeh, W.J. Choi, and K.N. Tu, *Appl. Phys. Lett.* 80, 4 (2002).
7. W.J. Choi, E.C.C. Yeh, and K.N. Tu, *J. Appl. Phys.* 94, 5665 (2003).
8. T.L. Shao, S.H. Chiu, Chih Chen, D.J. Yao, and C.Y. Hsu, *J. Electron. Mater.* 33, 1350 (2004).
9. J.W. Nah, K.W. Paik, J.O. Suh, and K.N. Tu, *J. Appl. Phys.* 94, 7560 (2003).
10. T.L. Shao, Y.H. Chen, S.H. Chiu, and Chih Chen, *J. Appl. Phys.* 96, 4518 (2004).
11. S.Y. Jang, J. Wolf, W.S. Kwon, and K.W. Paik, Proc. 52th Electronic Components and Technology Conf. (San Diego, CA: IEEE Components, Packaging, and Manufacturing Technology Society, 2002), p. 1213.
12. S.W. Liang, T.L. Shao, Chih Chen, C.C. Everett Yeh, and K.N. Tu, *J. Mater. Res.* 21, 137 (2006).
13. N.F. Mott and H. Jones *The Theory of the Properties of Metals and Alloys* Dover, (New York, NY, 1958), p. 242.
14. T.L. Shao, S.W. Liang, T.C. Lin, and Chih Chen, *J. Appl. Phys.* 98, 044509 (2005).
15. Hua Ye, Cemal Basaran, and Douglas Hopkins, *Appl. Phys. Lett.* 82, 7 (2003).
16. J.R. Black, *IEEE Trans. Electron Dev.* ED-164, 338 (1969).
17. H. Balkan, *Proc. 54th Electronic Components and Technology Conf.* (Las Vegas, NV: IEEE Components, Packaging, and Manufacturing Technology Society, 2004), p. 893.
18. J.D. Wu, C.W. Lee, P.J. Zheng, J.C.B. Lee, and S. Li Proc. 54th Electronic Components and Technology Conf IEEE Components, Packaging, and Manufacturing Technology Society, (Las Vegas, NV, 2004), p. 961.
19. Yi-Shao Lai, Kuo-Ming Chen, Chiu-Wen Lee, Chin-Li Kao, and Yu-Hsiu Shao, *Proc. 7th Electronic Packaging Technology Conf.* (Singapore: IEEE Components, Packaging, and Manufacturing Technology Society, Singapore, 2005), p. 786.
20. S.H. Chiu, T.L. Shao, Chih Chen, D.J. Yao, and C.Y. Hsu, *Appl. Phys. Lett.* 88, 022110 (2006).